

Identifying the chemical and structural irreversibility in $\text{LiNi}_{0.8}\text{Co}_{0.15}\text{Al}_{0.05}\text{O}_2$ - A model compound for classical layered intercalation

Haodong Liu^a, Hao Liu^b, Ieuan D. Seymour^c, Natasha Chernova^d, Kamila M. Wiaderek^b, Nicole M. Trease^c, Sunny Hy^a, Yan Chen^e, Ke An^e, Minghao Zhang^a, Olaf J. Borkiewicz^b, Saul H. Lapidus^b, Bao Qiu^f, Yonggao Xia^f, Zhaoping Liu^f, Peter J. Chupas^b, Karena W Chapman^b, M. Stanley Whittingham^d, Clare P. Grey^c, Ying Shirley Meng^{a*}

a. Department of NanoEngineering, University of California San Diego, 9500 Gilman Drive, La Jolla, California 92093, USA *Email - shirleymeng@ucsd.edu, shirleymeng@gmail.com

b. X-ray Science Division, Advanced Photon Source, Argonne National Laboratory, Argonne, Illinois 60439, USA

c. Department of Chemistry, University of Cambridge, Lensfield Road, Cambridge, CB2 1EW, UK

d. Institute for Materials Research, SUNY Binghamton, Binghamton, New York 13902-6000, USA

e. Chemical and Engineering Materials Division, Oak Ridge National Laboratory, Oak Ridge, Tennessee 37830, USA

f. Advanced Li-ion Battery Engineering Laboratory and Key Laboratory of Graphene Technologies and Applications of Zhejiang Province, Ningbo Institute of Materials Technology & Engineering (NIMTE), Chinese Academy of Sciences, Ningbo, Zhejiang 315201, P. R. China

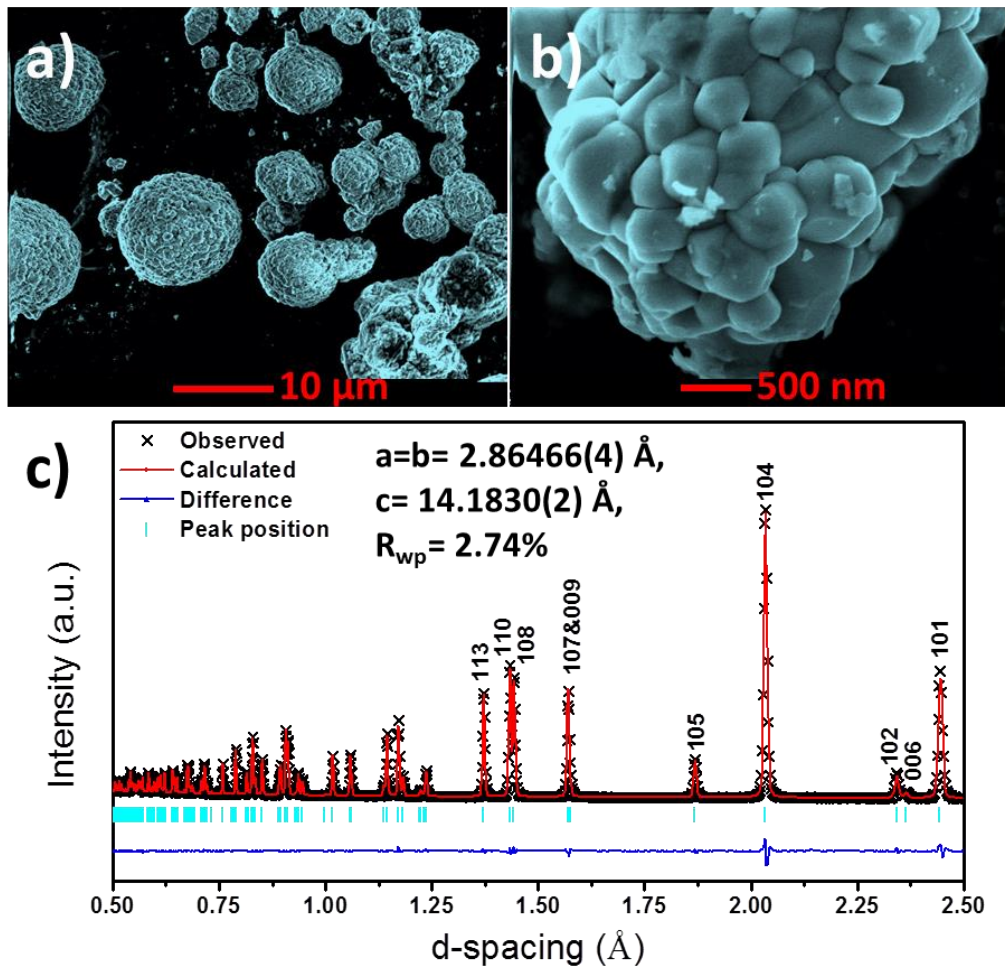


Figure S1. a) and b) SEM of NCA. c) Neutron powder diffraction of NCA.

Table S1. Neutron diffraction data refinement results of NCA pristine powders.

Pristine, Space Group: $R\bar{3}m$						
$a=b= 2.86466(4) \text{ \AA}, c= 14.1830(2) \text{ \AA}$, Neutron: $R_{wp}= 2.74\%$						
Atom type	x	y	z	Occupancy	100*U (\AA^2)	
Li	0	0	0	0.010(2)	$U_{11}=U_{22}= 0.41(2)$	$U_{33}= 0.27(3)$
Ni	0	0	0	0.790(2)	$U_{11}=U_{22}= 0.41(2)$	$U_{33}= 0.27(3)$
Co	0	0	0	0.150	$U_{11}=U_{22}= 0.41(2)$	$U_{33}= 0.27(3)$
Al	0	0	0	0.050	$U_{11}=U_{22}= 0.41(2)$	$U_{33}= 0.27(3)$
Li	0	0	0.5	0.990(2)	$U_{iso}= 1.40(6)$	
Ni	0	0	0.5	0.010(2)	$U_{iso}= 1.40(6)$	
O	0	0	0.25936(4)	1.000	$U_{iso}= 0.95(2)$	

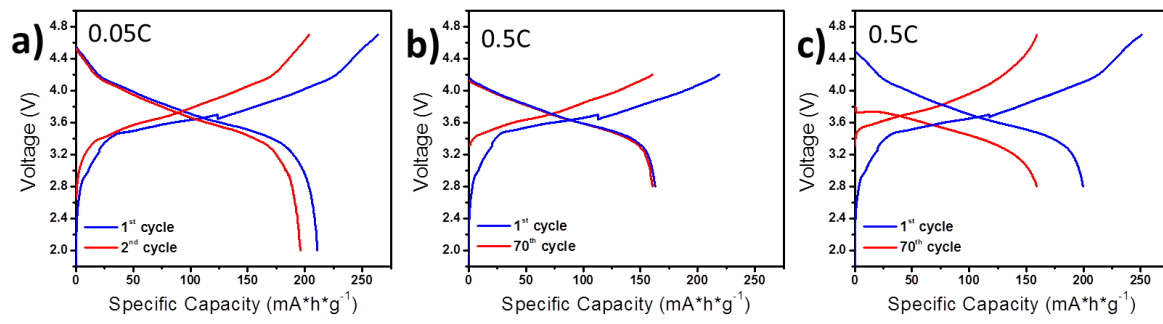


Figure S2. Voltage profiles of NCA pouch cell (vs. graphite). a) 2.0 -4.7 V, C/20. b) 2.8 -4.2 V, C/2. c) 2.8-4.7V, C/2.

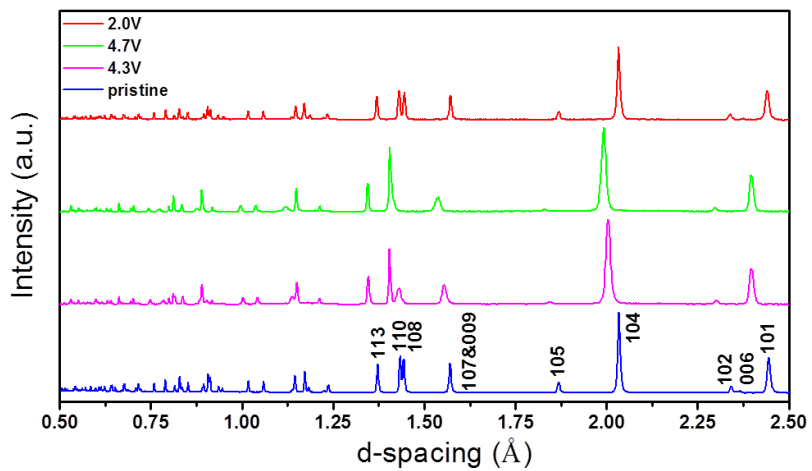


Figure S3. Neutron diffraction patterns of NCA at different states of (dis)charge during the 1st cycle.

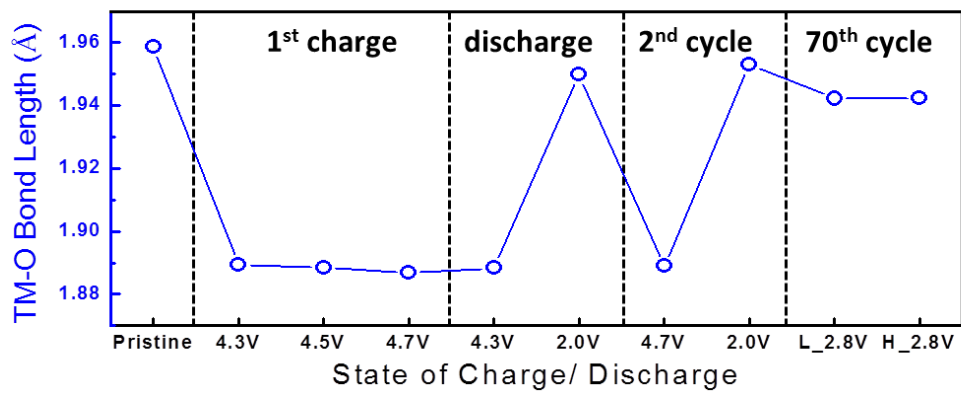


Figure S4. The TM-O bond length obtained from X-ray and Neutron diffraction joint refinement.

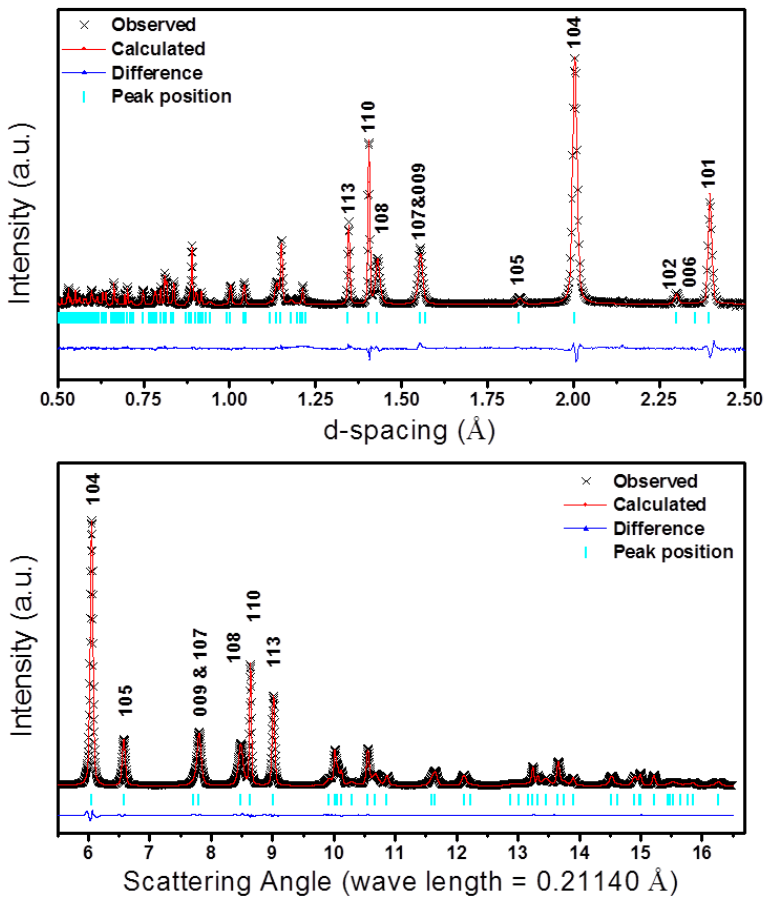


Figure S5. X-ray and Neutron diffraction data joint refinement of NCA at 1st cycle 4.3V charged state. Neutron (upper) and X-ray (lower).

Table S2. X-ray and Neutron diffraction data joint refinement results of NCA at 1st cycle 4.3V charged state.

1 st cycle 4.3V, Space Group: $\bar{R}\bar{3}m$						
a=b= 2.80623(4) Å, c= 14.1331(4) Å,						
X-ray: R_{wp} = 3.80%, Neutron: R_{wp} = 3.66%						
Atom type	x	y	z	Occupancy	$100^*U (\text{\AA}^2)$	
Li	0	0	0	0.000	$U_{11}=U_{22}= 0.26(1)$	$U_{33}= 1.23(3)$
Ni	0	0	0	0.784(1)	$U_{11}=U_{22}= 0.26(1)$	$U_{33}= 1.23(3)$
Co	0	0	0	0.150	$U_{11}=U_{22}= 0.26(1)$	$U_{33}= 1.23(3)$
Al	0	0	0	0.050	$U_{11}=U_{22}= 0.26(1)$	$U_{33}= 1.23(3)$
Li	0	0	0.5	0.166(14)	$U_{iso}= 1.58(35)$	
Ni	0	0	0.5	0.016(1)	$U_{iso}= 1.58(35)$	
O	0	0	0.26455(5)	1.000	$U_{iso}= 0.86(2)$	

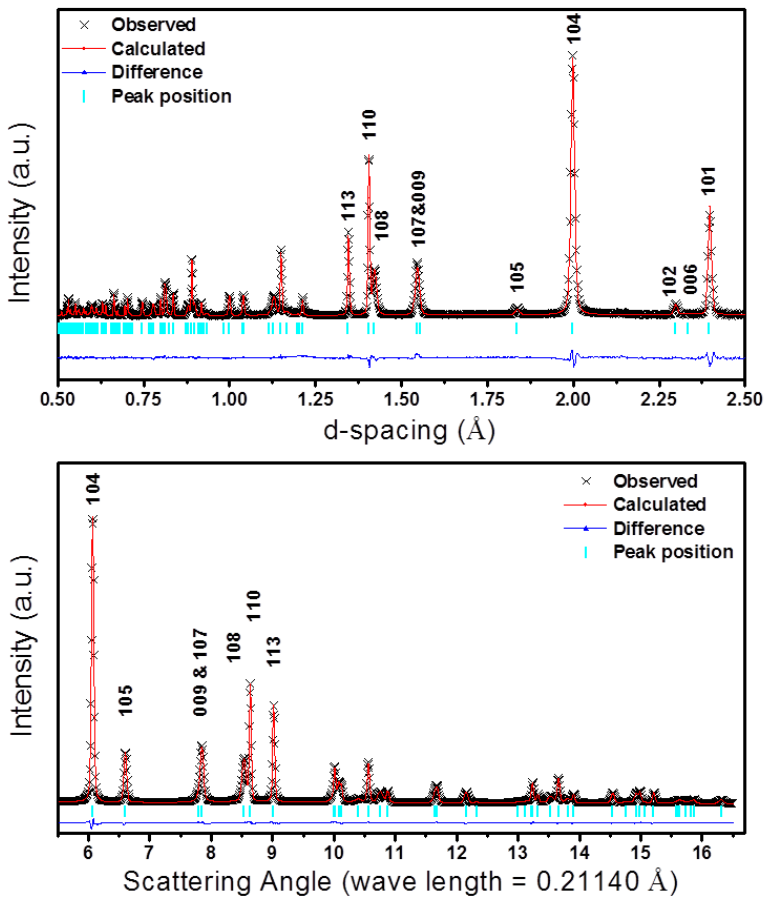


Figure S6. X-ray and Neutron diffraction data joint refinement of NCA at 1st cycle 4.5V charged state. Neutron (upper) and X-ray (lower).

Table S3. X-ray and Neutron diffraction data joint refinement results of NCA at 1st cycle 4.5V charged state.

1 st cycle 4.5V, Space Group: R̄3m a=b= 2.80717(3) Å, c= 13.9972(3) Å, X-ray: R _{wp} = 2.72%, Neutron: R _{wp} = 3.59%						
Atom type	x	y	z	Occupancy	100*U (Å ²)	
Li	0	0	0	0.000	U11=U22= 0.26(1)	U33= 1.76(3)
Ni	0	0	0	0.784(1)	U11=U22= 0.26(1)	U33= 1.76(3)
Co	0	0	0	0.150	U11=U22= 0.26(1)	U33= 1.76(3)
Al	0	0	0	0.050	U11=U22= 0.26(1)	U33= 1.76(3)
Li	0	0	0.5	0.147(17)	Uiso= 2.43(46)	
Ni	0	0	0.5	0.016(1)	Uiso= 2.48(46)	
O	0	0	0.26406(6)	1.000	Uiso= 0.89(2)	

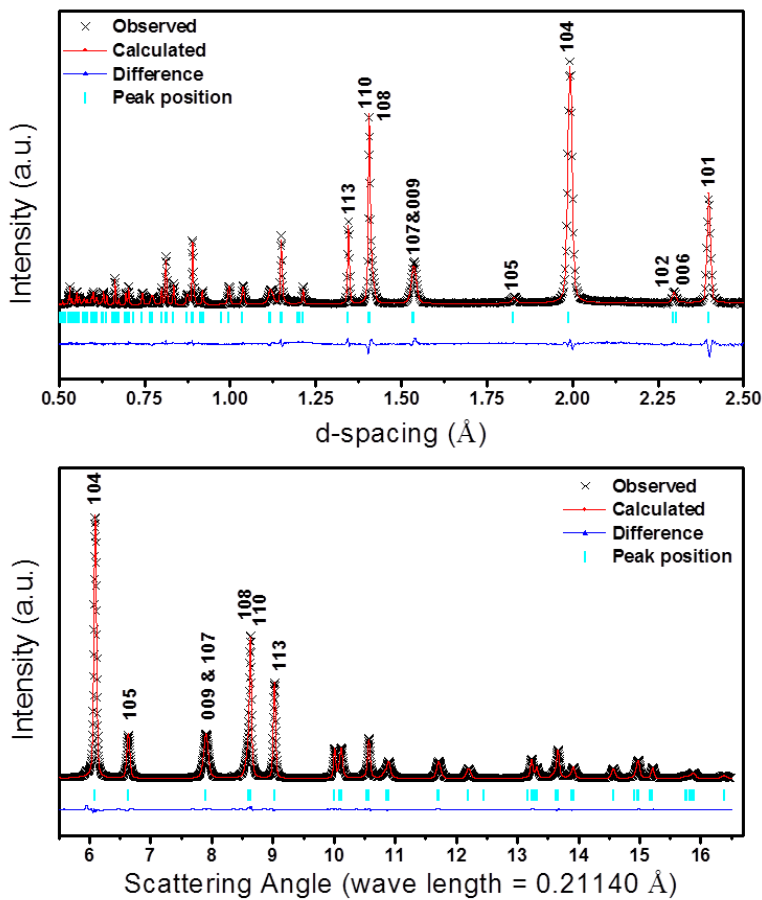


Figure S7. X-ray and Neutron diffraction data joint refinement of NCA at 1st cycle 4.7V charged state. The ADP parameters of transition metals are set as isotropic. Neutron (upper) and X-ray (lower).

Table S4. X-ray and Neutron diffraction data joint refinement results of NCA at 1st cycle 4.7V charged state.

Atom type	x	y	z	Occupancy	100*U (Å ²)	
					U ₁₁ =U ₂₂	U ₃₃
Li	0	0	0	0.000	0.18(1)	1.90(4)
Ni	0	0	0	0.786(1)	0.18(1)	1.90(4)
Co	0	0	0	0.150	0.18(1)	1.90(4)
Al	0	0	0	0.050	0.18(1)	1.90(4)
Li	0	0	0.5	0.097(12)	U _{iso} = 1.79(23)	
Ni	0	0	0.5	0.014(1)	U _{iso} = 1.79(23)	
O	0	0	0.26355(6)	1.000	U _{iso} = 0.81 (2)	

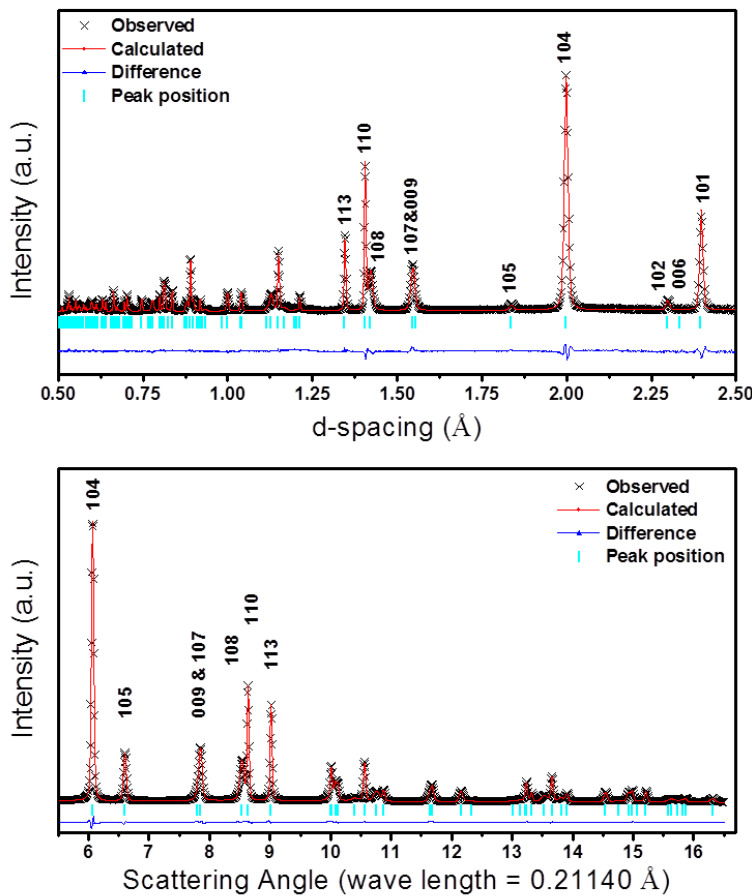


Figure S8. X-ray and Neutron diffraction data joint refinement of NCA at 1st cycle 4.3V discharged state. Neutron (upper) and X-ray (lower).

Table S5. X-ray and Neutron diffraction data joint refinement results of NCA at 1st cycle 4.3V discharged state.

1 st cycle 4.3V (discharge), Space Group: R̄3m a=b= 2.80728(4) Å, c= 13.9942(4) Å, X-ray: R _{wp} = 2.70%, Neutron: R _{wp} = 3.62%						
Atom type	x	y	z	Occupancy	100*U (Å ²)	
Li	0	0	0	0.000	U11=U22= 0.26(1)	U33= 1.76 (3)
Ni	0	0	0	0.784(1)	U11=U22= 0.26(1)	U33= 1.76 (3)
Co	0	0	0	0.150	U11=U22= 0.26(1)	U33= 1.76 (3)
Al	0	0	0	0.050	U11=U22= 0.26(1)	U33= 1.76 (3)
Li	0	0	0.5	0.143(17)	Uiso= 2.47(46)	
Ni	0	0	0.5	0.016(1)	Uiso= 2.47(46)	
O	0	0	0.26408(6)	1.000	Uiso= 0.88 (2)	

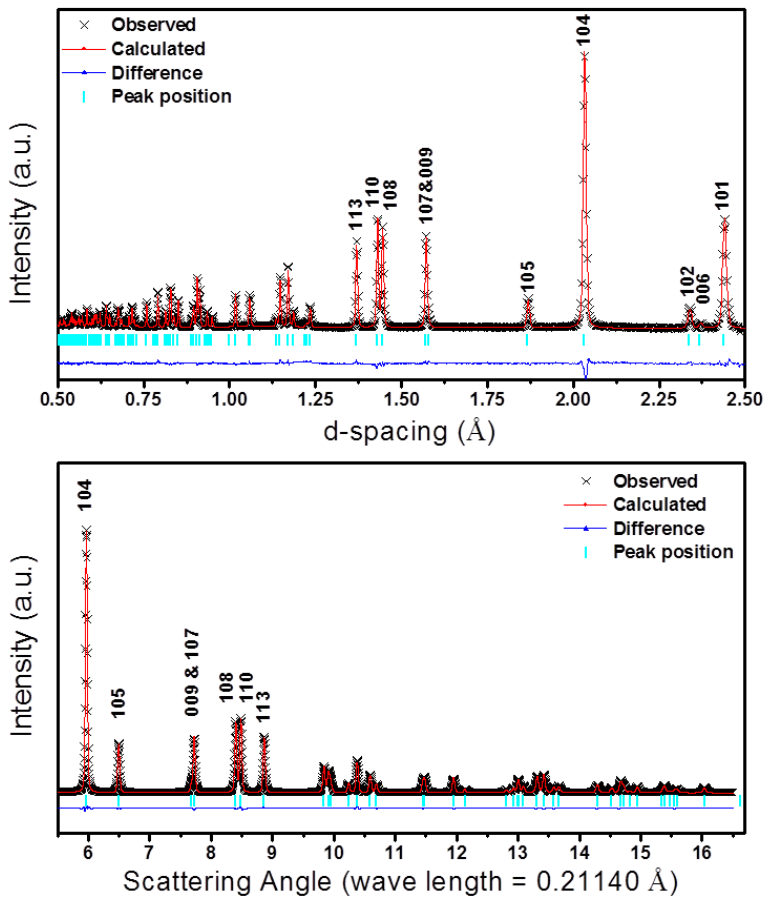


Figure S9. X-ray and Neutron diffraction data joint refinement of NCA at 1st cycle 2.0V discharged state. Neutron (upper) and X-ray (lower).

Table S6. X-ray and Neutron diffraction data joint refinement results of NCA at 1st cycle 2.0V discharged state.

1 st cycle 2.0V, Space Group: R̄3m a=b= 2.85742(2) Å, c= 14.2106 (1) Å, X-ray: Rwp= 2.51%, Neutron: Rwp= 3.18%						
Atom type	x	y	z	Occupancy	100*U (Å ²)	
Li	0	0	0	0.000	U11=U22= 0.30(1)	U33= 0.45(1)
Ni	0	0	0	0.784(1)	U11=U22= 0.30(1)	U33= 0.45(1)
Co	0	0	0	0.150	U11=U22= 0.30(1)	U33= 0.45(1)
Al	0	0	0	0.050	U11=U22= 0.30(1)	U33= 0.45(1)
Li	0	0	0.5	0.883(8)	Uiso= 1.27(3)	
Ni	0	0	0.5	0.016(1)	Uiso= 1.27(3)	
O	0	0	0.26019(3)	1.000	Uiso= 1.02(1)	

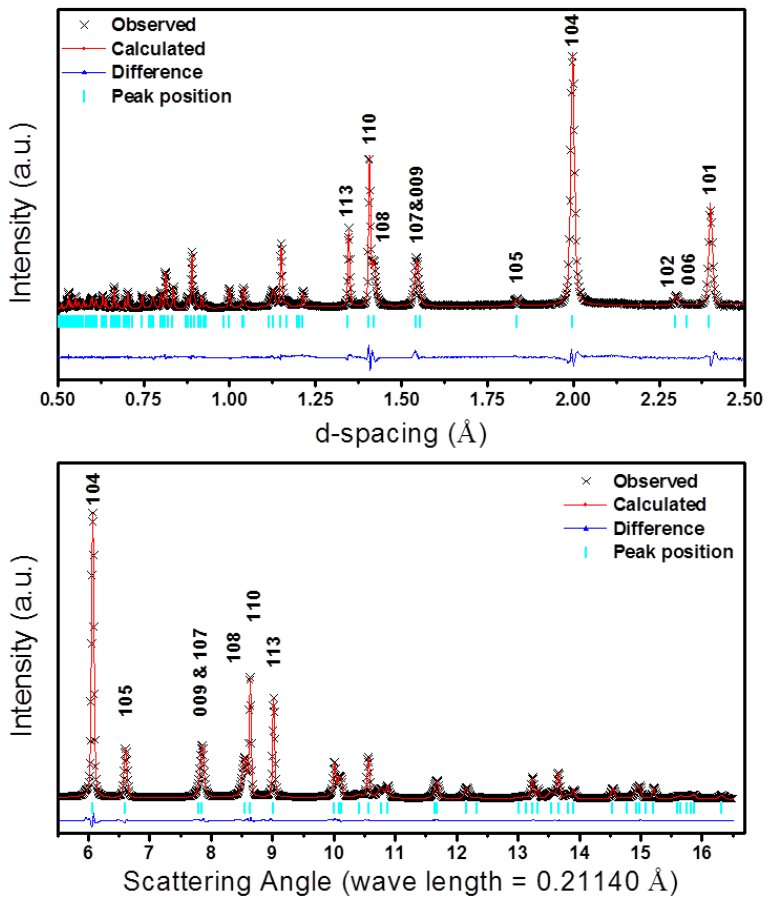


Figure S10. X-ray and Neutron diffraction data joint refinement of NCA at 2nd cycle 4.7V charged state. Neutron (upper) and X-ray (lower).

Table S7. X-ray and Neutron diffraction data joint refinement results of NCA at 2nd cycle 4.7V charged state.

2 nd cycle 4.7V, Space Group: R̄3m a=b= 2.80756(4) Å, c= 13.9783(5) Å, X-ray: R _{wp} = 3.37%, Neutron: R _{wp} = 3.77%						
Atom type	x	y	z	Occupancy	100*U (Å ²)	
Li	0	0	0	0.000	U11=U22= 0.29(2)	U33= 1.78(4)
Ni	0	0	0	0.784(1)	U11=U22= 0.29(2)	U33= 1.78(4)
Co	0	0	0	0.150	U11=U22= 0.29(2)	U33= 1.78(4)
Al	0	0	0	0.050	U11=U22= 0.29(2)	U33= 1.78(4)
Li	0	0	0.5	0.138(20)	Uiso= 2.25(55)	
Ni	0	0	0.5	0.016(1)	Uiso= 2.25(55)	
O	0	0	0.26394(7)	1.000	Uiso= 0.93(3)	

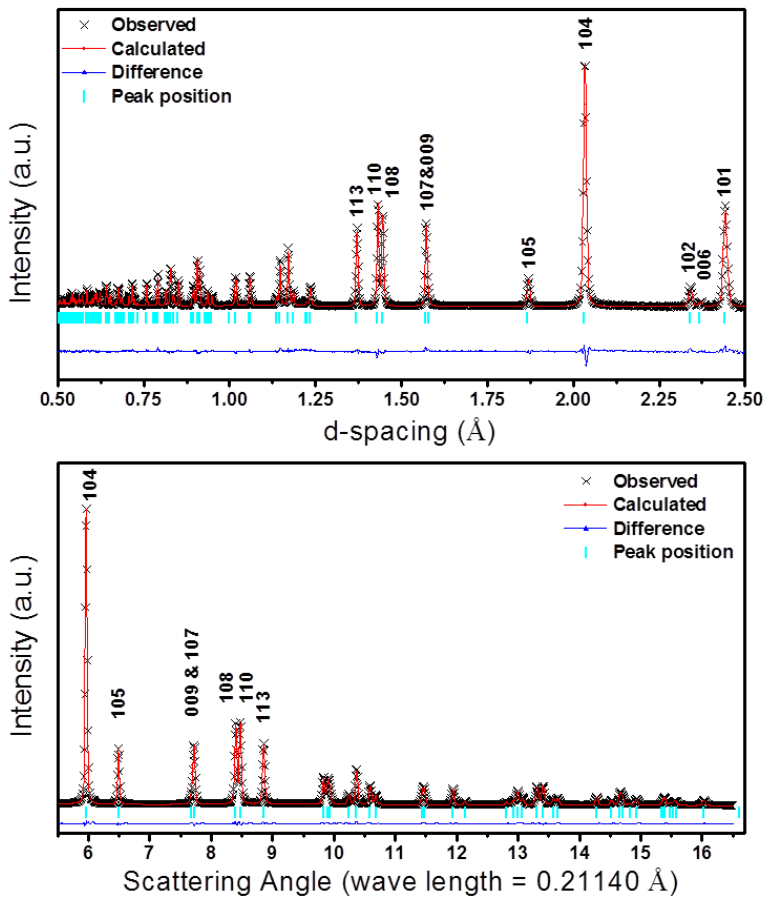


Figure S11. X-ray and Neutron diffraction data joint refinement of NCA at 2nd cycle 2.0V discharged state. Neutron (upper) and X-ray (lower).

Table S8. X-ray and Neutron diffraction data joint refinement results of NCA at 2nd cycle 2.0V discharged state.

2 nd cycle 2.0V, Space Group: $\bar{R}\bar{3}m$						
a=b= 2.86075(3) Å, c= 14.2067(2) Å,						
X-ray: R_{wp} = 2.53%, Neutron: R_{wp} = 3.19%						
Atom type	x	y	z	Occupancy	100*U (\AA^2)	
Li	0	0	0	0.000	U11=U22= 0.34(2)	U33= 0.48(1)
Ni	0	0	0	0.782(2)	U11=U22= 0.34(2)	U33= 0.48(1)
Co	0	0	0	0.150	U11=U22= 0.34(2)	U33= 0.48(1)
Al	0	0	0	0.050	U11=U22= 0.34(2)	U33= 0.48(1)
Li	0	0	0.5	0.906(10)	Uiso= 1.24(4)	
Ni	0	0	0.5	0.018(2)	Uiso= 1.24(4)	
O	0	0	0.25994(4)	1.000	Uiso= 1.05(2)	

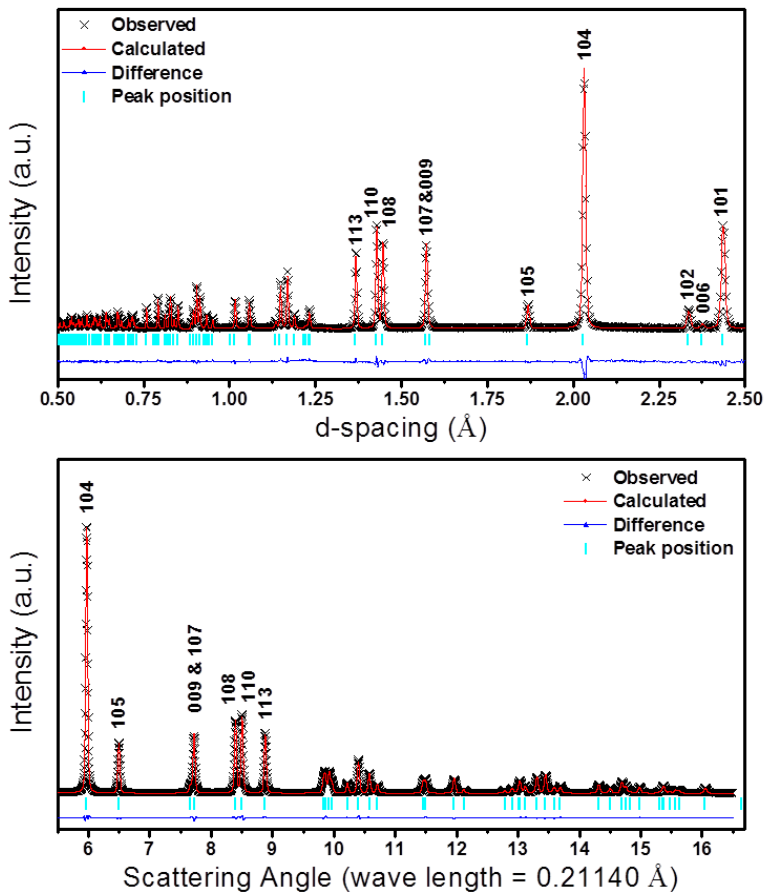


Figure S12. X-ray and Neutron diffraction data joint refinement of NCA at 70th cycle 2.8V discharged state. Neutron (upper) and X-ray (lower).

Table S9. X-ray and Neutron diffraction data joint refinement results of NCA at 70th cycle 2.8V discharged state.

70 th cycle 2.8-4.2V discharged, Space Group: R̄3m a=b= 2.85095(2) Å, c= 14.2402(1) Å, X-ray: Rwp= 3.12%, Neutron: Rwp= 3.30%						
Atom type	x	y	z	Occupancy	100*U (Å ²)	
Li	0	0	0	0.000	U11=U22= 0.28(1)	U33= 0.47(1)
Ni	0	0	0	0.785(1)	U11=U22= 0.28(1)	U33= 0.47(1)
Co	0	0	0	0.150	U11=U22= 0.28(1)	U33= 0.47(1)
Al	0	0	0	0.050	U11=U22= 0.28(1)	U33= 0.47(1)
Li	0	0	0.5	0.814 (9)	Uiso= 1.34(4)	
Ni	0	0	0.5	0.015(1)	Uiso= 1.34(4)	
O	0	0	0.26092(4)	1.000	Uiso= 0.98(2)	

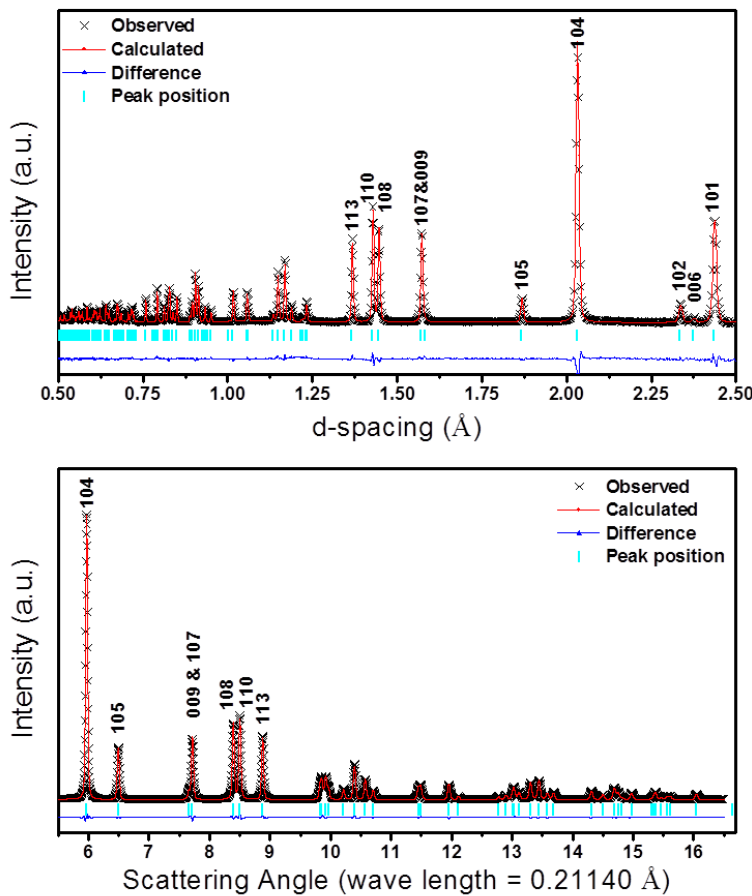


Figure S13. X-ray and Neutron diffraction data joint refinement of NCA at 70th cycle 2.8V discharged state. Neutron (upper) and X-ray (lower).

Table S10. X-ray and Neutron diffraction data joint refinement results of NCA at 70th cycle 2.8V discharged state.

70 th cycle 2.8-4.7V discharged, Space Group: R̄3m a=b= 2.85174(2) Å, c= 14.2461(1) Å, X-ray: Rwp= 3.28%, Neutron: Rwp= 3.25%						
Atom type	x	y	z	Occupancy	100*U (Å ²)	
Li	0	0	0	0.000	U11=U22= 0.28(1)	U33= 0.52(1)
Ni	0	0	0	0.779(1)	U11=U22= 0.28(1)	U33= 0.52(1)
Co	0	0	0	0.150	U11=U22= 0.28(1)	U33= 0.52(1)
Al	0	0	0	0.050	U11=U22= 0.28(1)	U33= 0.52(1)
Li	0	0	0.5	0.787(10)	Uiso= 1.49(4)	
Ni	0	0	0.5	0.021(1)	Uiso= 1.49(4)	
O	0	0	0.26099(4)	1.000	Uiso= 1.03(2)	

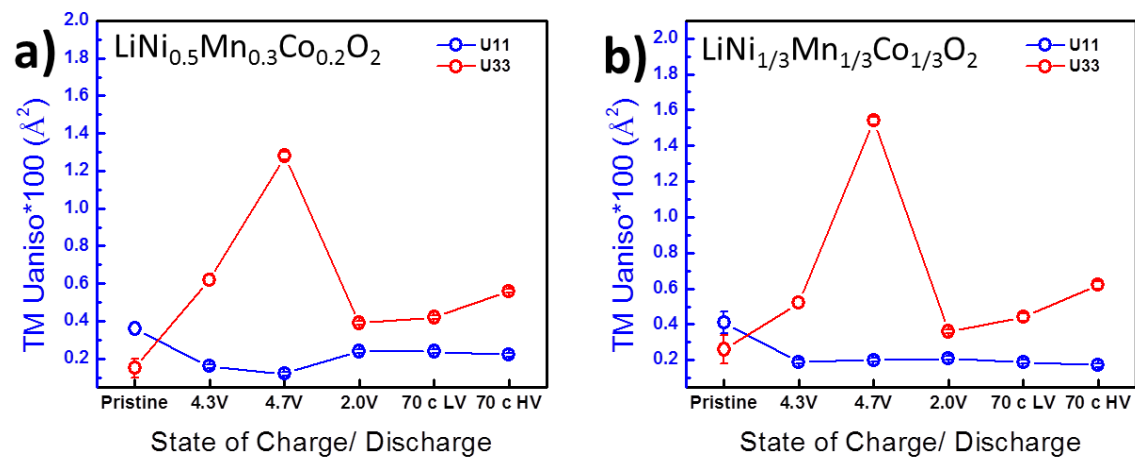


Figure S14. Atomic displacement parameters from X-ray and Neutron diffraction data joint refinement. a) $\text{LiNi}_{0.5}\text{Mn}_{0.3}\text{Co}_{0.2}\text{O}_2$; b) $\text{LiNi}_{1/3}\text{Mn}_{1/3}\text{Co}_{1/3}\text{O}_2$.

Modeling the ${}^7\text{Li}$ NMR spectra of cycled NCA

The ${}^7\text{Li}$ NMR spectra of $\text{Li}_x\text{Ni}_{0.8}\text{Co}_{0.15}\text{Al}_{0.05}\text{O}_2$ at different states of discharge were modeled with a simple random solution model similar to the one used in ref.¹ The ${}^7\text{Li}$ spectrum of delithiated NCA depends on the number of paramagnetic Ni^{3+} ions in the nearest neighbor (nn) and next nearest neighbor (nnn) environments that form 90° and 180° Li-O-Ni³ bond pathways, respectively. For a dynamic Jahn-Teller distortion, the rapid averaging of the Jahn-Teller lengthened and Jahn-Teller shortened Ni-O bonds means that only a single contribution to the ${}^7\text{Li}$ shift is expected for each Li-O-Ni³ bond pathway as discussed in ref.²

In total there are $6 \times 90^\circ$ Li-O-M (nn) and $6 \times 180^\circ$ Li-O-M bond pathway configurations, where M=Ni³⁺, Ni⁴⁺, Al³⁺ and Co³⁺. To simplify the model, it was assumed that only $\text{Ni}^{3+} \rightarrow \text{Ni}^{4+}$ oxidation was occurring and so the probability of a metal species P_M being in a nn or nnn environment around Li is given by the Li composition (x) as $P_{\text{Ni}^{3+}} = (x - 0.2)$, $P_{\text{Ni}^{4+}} = (1 - x)$, $P_{\text{Co}^{3+}} = 0.15$ and $P_{\text{Al}^{3+}} = 0.05$.

The total probability f_{Li} of a Li site having k Ni³⁺ neighbors in the 6 nn and 6 nnn sites is given by;

$$f_{Li, \text{Ni}^{3+}} = \binom{6}{k_{nn}} \binom{6}{k_{nnn}} (P_{\text{Ni}^{3+}})^{k_{nn} + k_{nnn}} (1 - P_{\text{Ni}^{3+}})^{12 - k_{nn} - k_{nnn}}$$

where:

$$\binom{6}{k} = \frac{6!}{k! (6 - k)!}$$

For each possible Li configuration the Fermi contact shift, δ , is calculated by summing up the individual ${}^7\text{Li}$ Li-O-M bond pathway contributions. Dynamically Jahn-Teller averaged ${}^7\text{Li}$ NMR bond pathway contributions of -15 and 110 ppm obtained from a previous experimental study were used for the 90° and 180° Li-O-Ni³⁺ bond pathways, respectively, and all other Li-O-M pathway contributions were assumed to be 0 ppm.³ The overall ${}^7\text{Li}$ spectrum was calculated by modeling each Li environment with shift, δ , and intensity, $f_{Li, \text{Ni}^{3+}}$, with a Gaussian peak of width 60 ppm. The model spectra at different states of discharge corresponding to experimentally observed compositions, i.e. $x = 1$ (pristine), $x = 0.85$ (1st discharge to 2 V), $x = 0.8$ (70 cycles low voltage window) and $x = 0.71$ (70 cycles high voltage window) are shown in Figure S15.

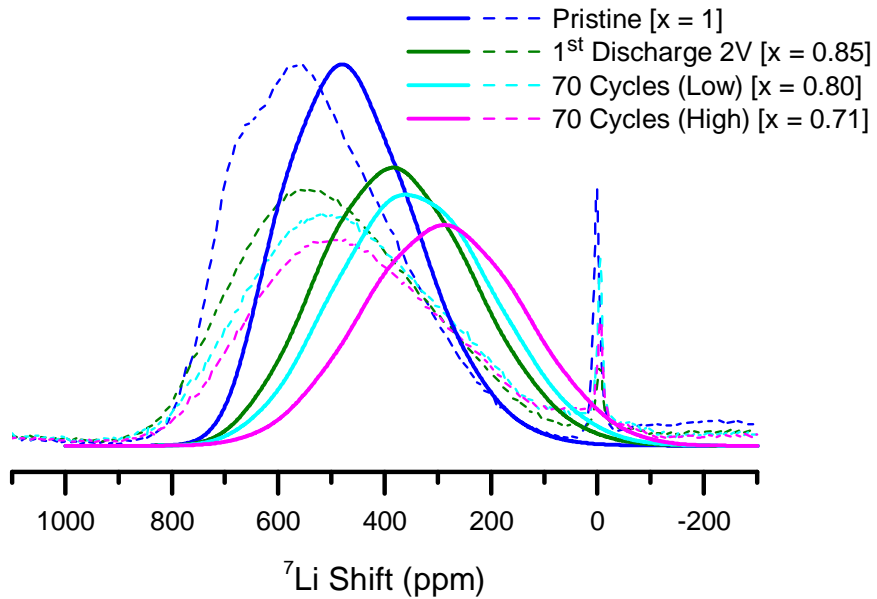


Figure S15 Comparison of experimental ${}^7\text{Li}$ NMR spectra (dashed lines) and model spectra (solid lines) of $\text{Li}_x\text{Ni}_{0.8}\text{Co}_{0.15}\text{Al}_{0.05}\text{O}_2$ cycled to different discharged states (x). The model spectra were produced with a random solution model in which $M = (x-0.2) \text{ Ni}^{3+}, (1-x) \text{ Ni}^{4+}, 0.05 \text{ Al}^{3+}$ and 0.15 Co^{3+} ions were randomly distributed in the $6 \times 90^\circ$ Li-O-M (nearest neighbor) and $6 \times 180^\circ$ Li-O-M (next nearest neighbor) environments around Li. Dynamic Jahn-Teller averaged ${}^7\text{Li}$ NMR bond pathway contributions of -15 and 110 ppm were used for the 90° and 180° Li-O-Ni $^{3+}$ bond pathways, respectively. Each Li resonance in the random solution model was modeled with a Gaussian peak with a width of 60 ppm.

It can be seen from Figure S15 that although the absolute value of the ${}^7\text{Li}$ shift is underestimated in the model spectra, the systematic decrease in the ${}^7\text{Li}$ NMR shift with Li content (x), as result of $\text{Ni}^{3+} \rightarrow \text{Ni}^{4+}$ oxidation is well represented. The difference in the experimentally observed and modeled ${}^7\text{Li}$ NMR shifts may in part be related to the magnitude of the bond pathway contributions used which were taken from the Co-rich phase of $\text{LiNi}_{0.3}\text{Co}_{0.7}\text{O}_2$.³ The simple random solution model in this work also does not include any effects of Li and Ni $^{3+}$ /Ni $^{4+}$ ordering or $\text{Co}^{3+} \rightarrow \text{Co}^{4+}$ oxidation, which may lead to slight deviations in the distribution. However, even without these additional effects, the simple model used in this work does suggest that the variation in the ${}^7\text{Li}$ spectrum after extended cycling is predominantly due to the differences in Li content/ Ni-oxidation state instead of from extensive structural rearrangement of Co, Al and Ni.

Table S11. Magnetic parameters of NCA samples at different cycling stages.

Sample	C_M , emu K/ mol TM	Θ , K	$\chi_0, 10^{-4}$ emu/mol TM	M_R , emu/ mol TM	T_f , K	μ_{exp}, μ_B	$\mu_{theor},$ μ_B
pristine	0.489(1)	17.1(1)	2.0	9.2	6.5	1.98	1.60
4.3 V ch1	0.016(1)	-4.3(6)	1.9	0.20	-	0.36	0.33
4.5 V ch1	0.021(1)	-12.6(4)	2.8	0.16	-	0.41	0.41
4.7 V ch1	0.027(3)	-5.3(3)	2.8	0.15	-	0.47	0.57
4.7 V ch2	0.021(1)	2.8(1)	2.1	0.27	-	0.41	0.44
4.3 V dis1	0.021(1)	-7.0(2)	2.6	0.22	-	0.41	0.42
2.0 V dis1	0.354(1)	27.1(1)	1.0	16.5	6.5 and 100	1.68	1.47
2.0 V dis2	0.363(1)	27.4(1)	3.0	20.6	6.5 and 100	1.70	1.49
2.8 V 70L	0.344(1)	21.8(2)	3.0	19.6	6.5 and 100	1.66	1.39
2.8 V 70H	0.324(1)	24.1(1)	3.8	17.1	6.5 and 100	1.61	1.36

1. N. M. Trease, I. D. Seymour, M. D. Radin, H. Liu, H. Liu, S. Hy, N. Chernova, P. Parikh, A. Devaraj, K. M. Wiaderek, P. J. Chupas, K. W. Chapman, M. S. Whittingham, Y. S. Meng, A. Van der Van and C. P. Grey, *Chem Mater*, 2016, **28**, 8170-8180.
2. D. S. Middlemiss, A. J. Ilott, R. J. Clement, F. C. Strobridge and C. P. Grey, *Chem Mater*, 2013, **25**, 1723-1734.
3. D. Carlier, M. Menetrier and C. Delmas, *J Mater Chem*, 2001, **11**, 594-603.